# Upgrading of Bio-oil in Supercritical Ethanol: Using Furfural and Acetic Acid as Model Compounds

Wen Chen, Zhongyang Luo,* Yi Yang, Guoxiang Li, Jixiang Zhang, and Qi Dang

The upgrading of bio-oil in supercritical ethanol was investigated using furfural and acetic acid as model compounds with the aim of exploring the reaction pathways. The effects of catalysts, temperature, cold $H_2$ pressure, and the presence of other compounds were studied. Based on products analysis, upgrading with Pt/HZSM-5 improved performance over Pd/HZSM-5 and Ru/HZSM-5. Moreover, the catalytic performance of Pt/HZSM-5 could be enhanced by adding Ni as a second metal. Complete conversion of acetic acid and 83.06% conversion of furfural were achieved at 320 °C and 1.0 MPa of cold $H_2$ pressure. The presence of acetone was found to increase the conversion of furfural. Through gas chromatography–mass spectrometry (GC-MS) analysis, the reaction pathways of furfural and acetic acid were clarified. It was concluded that it is possible to combine different reactions including esterification, hydrogenation, ring opening, isomerization, aldol condensation, and acetalization in supercritical ethanol.

*Keywords: Bio-oil; Upgrading; Ethanol; Furfural; Catalysts*

*Contact information: State Key Laboratory of Clean Energy Utilization, Zhejiang University, Hangzhou 310027, China; *Corresponding author: zyluo@zju.edu.cn*

## INTRODUCTION

Bio-oil derived from biomass fast pyrolysis has the potential to be a significant substitute for petroleum in the transportation fuel sector. However, bio-oil presents some deleterious properties such as high viscosity, high water content, high corrosiveness, low heating value, and low stability (Czernik and Bridgwater 2004). Therefore, bio-oil must be upgraded before its successful application in gasoline and diesel engines.

The undesirable properties of bio-oil are due to its high oxygen content. Generally, two catalytic upgrading routes to reduce the oxygen content have been considered: hydrodeoxygenation and catalytic cracking (Mortensen *et al.* 2011). Hydrodeoxygenation is a process that treats bio-oil at a moderate temperature and high $H_2$ pressure to exclude oxygen from bio-oil in the presence of heterogeneous catalysts. A variety of metal catalysts, including conventional catalysts for petroleum hydroprocessing and noble metal catalysts, have been applied in the hydrodeoxygenation of bio-oil (Ardiyanti *et al.* 2011; Wildschut *et al.* 2010; Wildschut *et al.* 2009). The hydrogen consumption in the hydrodeoxygenation of bio-oil increases rapidly with the degree of deoxygenation, which makes this process uneconomic. Additionally, other problems, such as catalyst deactivation and low liquid yield, hamper the application of this process. Catalytic cracking operates at atmospheric pressure without the existence of hydrogen. Gayubo *et al.* (2004a,b) conducted catalytic transformation of oxygenate components of biomass pyrolysis oil on HZSM-5 zeolite. Coke deposition presents the greatest problem in catalytic cracking.

In fact, some oxygenated molecules such as alcohols, ethers, and esters can be directly applied to internal combustion engines. Zheng and Lou (2009) proposed another approach to convert unstable and corrosive oxygenated components into stable and flammable oxygenated compounds, such as alcohols, ethers, and esters, by coupling various types of reactions in the upgrading process. This approach was used to upgrade bio-oil in supercritical monoalcohols with metal–acid bifunctional catalysts (Li *et al.* 2011a; Peng *et al.* 2009; Tang *et al.* 2009; Zhang *et al.* 2012). Peng *et al.* (2008, 2009) showed that upgrading bio-oil could be greatly facilitated in supercritical ethanol using acidic catalysts. Zhang *et al.* (2012) studied the effects of supercritical solvents and catalysts on the upgrading of bio-oil and concluded that the process in ethanol had better upgrading performance than in methanol. Besides, ethanol is a renewable solvent which can be converted from lignocellulosic biomass and it can be used as a gasoline additive. Therefore, in this work, supercritical ethanol was used as the reaction solvent. The critical point of ethanol is 243 °C and 6.38 MPa, which is lower than that of water and methanol.

Most of the previously reported work dealing with the upgrading of bio-oil in supercritical solvents mainly has focused on the effects of catalysts, solvents, and reaction conditions, while little attention has been paid to the reaction pathways of typical bio-oil components. To clarify the reaction pathways, the upgrading reactions of model compounds of bio-oil were carried out in supercritical ethanol. Metal–acid bifunctional catalysts, including Pt/HZSM-5, Ru/HZSM-5, Pd/HZSM-5, and bimetallic-acid catalyst Pt-Ni/HZSM-5, were tested to provide some information for catalyst selection in the upgrading of bio-oil. Pt, Pd, and Ru are metal catalysts with superior hydrogenation activity, and Ni can catalyze hydrogenation and cracking. HZSM-5 as the support is a kind of molecular sieve with acid sites.

Bio-oil is a complex mixture composed of acids, aldehydes, alcohols, esters, ethers, ketones, phenols, *etc.* (Zhang *et al.* 2007). Organic acids, mainly acetic acid, contribute to the corrosiveness of bio-oil, while the aldehydes cause the instability of bio-oil. For a better understanding of the reaction mechanisms with bifunctional catalysts, furfural and acetic acid, representing typical aldehydes and acids components, were selected as model compounds in this work. The reaction pathways of furfural and acetic acids in this process were clarified based on gas chromatography/mass spectrometry (GC-MS) analysis. The effects of reaction temperature and cold $H_2$ pressure were investigated in the range of 260 to 320 °C and 0.5 to 2.0 MPa, respectively. The influence of adding other typical compounds of bio-oil, such as water, acetone, and guaiacol, to the reaction system were also studied.

## EXPERIMENTAL

### Materials

Metal catalyst precursors, including $H_2PtCl_6{\cdot}6H_2O$, $PdCl_2$, $RuCl_3{\cdot}3H_2O$, and $Ni(NO_3)_2{\cdot}6H_2O$, were obtained from Sinopharm Chemical Reagent Co. and Aladdin Co. HZSM-5 type zeolite catalyst with a Si/Al ratio of 25 was used as the catalyst support. Acetic acid (>99.5%) from Sinopharm Chemical Reagent, furfural (99%) from Sigma-Aldrich, and 2-furanmethanol were employed as reactants. Anhydrous ethanol (≥99.5%) from Sinopharm Chemical Reagent was used as the solvent. All chemicals were used as received without further purification.

## Catalyst Preparation and Characterization

The catalysts 5% Pt/HZSM-5 (designated as PtH), 5% Pd/HZSM-5 (designated as PdH), and 5% Ru/HZSM-5 (designated as RuH) were prepared by incipient wetness impregnation of HZSM-5 using aqueous solutions of $H_2PtCl_6 \cdot 6H_2O$, $PdCl_2$, and $RuCl_3 \cdot 3H_2O$ as precursors, respectively, followed by drying overnight, calcination at 550 °C in air for 3 h, and reduction (400 °C) in flowing hydrogen for 3 h. The catalyst 2% Pt-10% Ni/HZSM-5 (designated as PNH) was prepared by incipient wetness co-impregnation with aqueous solutions of the corresponding metal precursors ($H_2PtCl_6 \cdot 6H_2O$ and $Ni(NO_3)_2 \cdot 6H_2O$), followed by drying overnight, calcination at 550 °C in air for 3 h, and reduction (450 °C) in flowing hydrogen for 3 h.

Nitrogen adsorption–desorption isotherms were measured by a Micromeritics TRISTAR 3020 system. The specific surface area and average pore diameter of the catalyst was calculated according to the Brunauer-Emmett-Teller (BET) method. The X-ray diffraction (XRD) analysis was conducted on an X'Pert PRO X-ray diffractometer using CuKα radiation over $2\theta$ ranges from 10° to 70°. STEM images were obtained on a Tecnai G2 F30 S-Twin electron microscope with an accelerating voltage of 300 kv. The average metal particle size was calculated by the Scherrer equation and measured from the STEM images.

## Experimental Procedures

All the experiments were carried out in a 100-mL batch stainless steel batch autoclave equipped with an electrical heating jacket and a mechanical overhead agitator. Temperature and pressure of the autoclave were measured online.

In a typical experiment, 40 mL ethanol, 2 mL furfural, 2 mL acetic acid, and 0.3 g reduced catalyst were added into the autoclave. To study the effects of other bio-oil representative components, another 1 mL water, acetone, and guaiacol were added to the liquid mixture, separately. Subsequently, the leakage test was conducted, followed by excluding air with $N_2$ and $H_2$ and building up the initial pressure (1.0 MPa) with $H_2$. Then, the reactor was heated to the reaction temperature (260 °C) and kept at the reaction temperature for 3 h. The reactor was cooled down in atmosphere after the reaction was finished. The agitator was stirred at the speed of 500 rpm for the duration of the process. After the reactor was cooled to room temperature, the liquid and solid products were recovered, and the mass balance was calculated according to the recovered liquid and catalysts. Then, the liquid products and solid products were separated by vacuum filtration and submitted to further analysis, while the gas products were discharged without further analysis. The mass balance was close to 90% for all of the experiments.

## Product Analysis

The liquid products were qualitatively analyzed by GC-MS (Agilent 5937) with a HP-5 column (0.25mm*30m*0.25μm). The injector temperature was 260 °C in split mode and with nitrogen as the carrier gas. The GC-MS oven temperature was 40 °C for 3 min, then it was heated to 180 °C at 4.0 °C/min, up to 260 °C at 10 °C/min, and held at 260 °C for 10 min. Compounds were identified by means of the National Institute of Standards and Technology (NIST) library. The relative content of reaction products was quantified by the area normalization method from the GC-MS spectrum. In this paper, stable oxygenated organic compounds—alcohols/ethers (except for ethyl ether, which originated from the etherification of ethanol), ketones, and esters—were defined as desired products, while other compounds such as aldehydes, acetals (unstable in acidic

environments), and acids were defined as undesired products. Based on the GC-MS spectrum, Yd was defined as the total area percentage of desired products in order to characterize the selectivity of the upgrading process. Acetic acid conversion (AC) and furfural conversion (FC) were quantified by GC (Agilent 7890) with a HP-5 column using the external standard method. The operating conditions of the GC (Agilent 7890) were the same as for the GC-MS. AC and FC are used to denote the conversion of acetic acid and furfural, respectively.

After pretreatment at 300 °C under nitrogen atmosphere for 30 min to remove the volatile materials absorbed on the micropores, the recovered catalysts were submitted to thermogravimetric (TG) analysis by a TGA/SDTA 851 thermogravimetric analyzer. The analysis was carried out in the range of 25 to 650 °C with a temperature ramp of 10.0 °C/min under flowing $O_2$ atmosphere. The gas flow rate was 50 mL/min. Coke deposition was defined as the quotient of mass loss of the recovered catalysts during TG analysis divided by the residual mass of the same sample after TG analysis.

## RESULTS AND DISCUSSION

### Catalyst Characterization

All of the nitrogen adsorption–desorption isotherms (shown in Fig. 1) of the catalysts exhibited the type-I isotherm with an H4-type hysteresis loop, demonstrating the existence of micropore and mesopore in the catalysts. The BET area and the average pore diameter of the catalysts are listed in Table 1.

The BET area of the three monometallic /HZSM-5 catalysts was more than 300 $m^2/g$, while it was 279 $m^2/g$ for the bimetallic/HZSM-5 catalyst PNH. The specific area of the catalysts decreased with the increasing metal load. The average pore diameter of the catalysts was in the range of 2.1 to 2.2 nm, which confirmed the existence of mesopores in the catalysts.

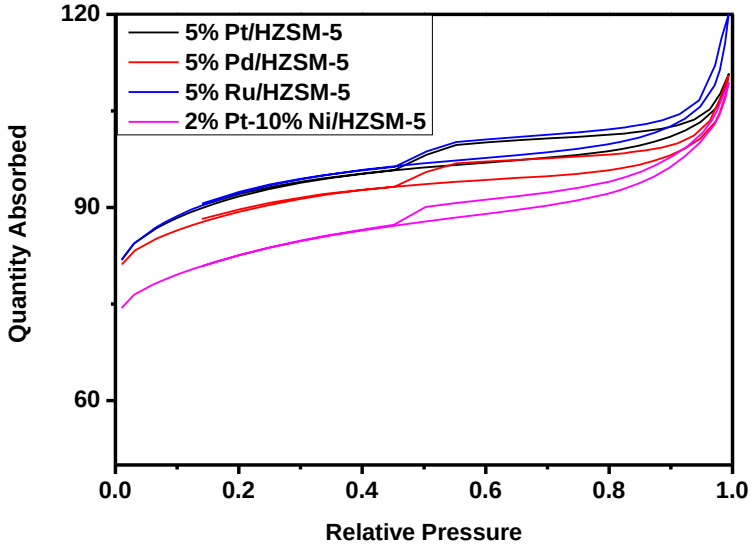


**Fig. 1.** $N_2$ adsorption–desorption isotherms of the catalysts

**Table 1.** Textural Properties of the Catalysts

| Catalysts | BET Area ($m^2$/g) | Pore Diameter (nm) | Average Metal Particle Size (nm)[a] | Average Metal Particle Size (nm)[b] |
|---|---|---|---|---|
| PtH[c] | 309 | 2.11 | 32.9 | 13.69 |
| PdH[d] | 300 | 2.13 | 41.9 | 44.81 |
| RuH[e] | 311 | 2.16 | 60.3 | 54.14 |
| PNH | 279 | 2.28 | 14.8 (NiO)[f] | 13.52 |

[a] Calculated from XRD patterns; [b] Measured from STEM images; [c] PtH, 5% Pt/HZSM-5; [d] PdH, 5% Pd/HZSM-5; [e] RuH, 5% Ru/HZSM-5; [f] PNH, 2% Pt 10% Ni/HZSM-5; no diffraction peaks corresponding to Pt crystallite

Figure 2 displays the XRD patterns of the catalysts. The XRD pattern of the PtH sample presented three intense diffraction peaks at $2\theta$ = 39.7°, 46.2°, and 67.4°, which could be attributed to the (111), (200), and (220) diffraction peaks of cubic Pt crystallite. Four diffraction peaks at $2\theta$ = 33.9°, 41.9°, 54.8°, and 60.2°, which could be indexed as the (101), (110), (112), and (103) reflections of the tetragonal PdO crystallite, were identified in the XRD pattern of PdH. Three diffraction peaks at $2\theta$ = 28.0°, 35.1°, and 54.3°, which corresponded with the standard diffraction peaks of tetragonal $RuO_2$ crystallite, were detected in the XRD patterns of RuH. In the XRD pattern of PNH, three diffraction peaks at $2\theta$ = 37.1°, 43.1°, and 62.6° corresponding to cubic NiO crystallite could be recognized. However, no diffraction peaks corresponding to Pt crystallite could be identified, indicating that Pt was highly dispersed in the PNH catalyst. Using the XRD patterns, the average metal particle size was calculated according to the Scherrer equation. The results together with the results obtained by STEM are displayed in Table 1. STEM images are shown in the Appendix (Fig. S1). The average particle size obtained from these two different methods was different. However, a similar trend was seen for the tested catalysts. PtH and PNH had smaller metal particles than PdH and RuH.

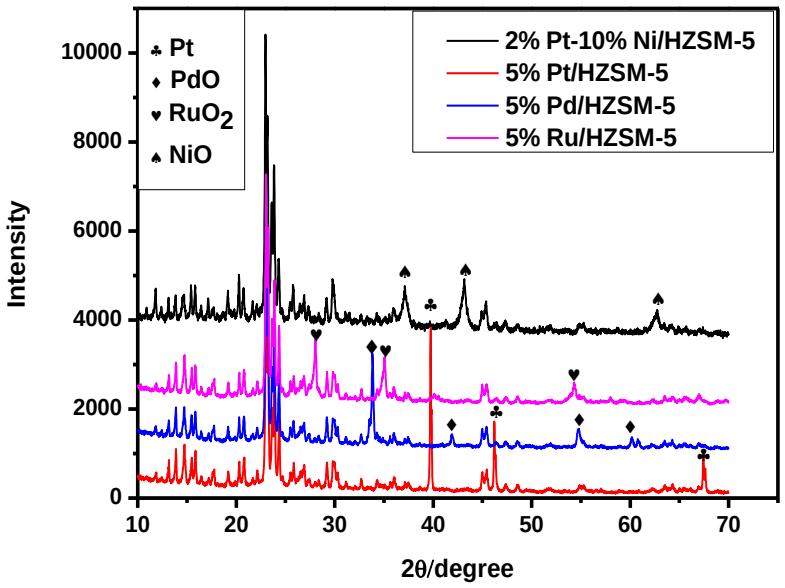


**Fig. 2.** XRD patterns of the catalysts

## Upgrading Performance and Effects of Catalysts

In this section, upgrading reactions were carried out at 260 °C and with 1.0 MPa of cold $H_2$ pressure with different catalysts. At this temperature, the system pressure was in the range of 7.0 to 7.5 MPa. It could be assumed that the ethanol (critical parameters, 243 °C and 6.38 MPa) in the reactor entered a supercritical state.

FC, AC, Yd, and coke deposition were used to compare the performance of upgrading reactions with different catalysts. Results are listed in Table 2. Complete conversion of acetic acid was achieved as no acetic acid was detected in the liquid products for all runs. The results were in accordance with the results obtained by Li *et al.* (2011b), which demonstrated that acetic acid could be totally converted in supercritical methanol even without the presence of catalysts. The conversion of furfural was sensitive to the catalysts. For the monometallic/HZSM-5 catalysts, the conversion of furfural using PtH was 62.94%, higher than the 44.01% using PdH and the 49.22% using RuH.

**Table 2.** Catalyst Catalytic Performance [a]

| | PtH[b] | PdH[c] | RuH[d] | PNH[e] |
|---|---|---|---|---|
| AC (%) | 100 | 100 | 100 | 100 |
| FC (%) | 62.94 | 44.01 | 49.22 | 73.56 |
| Yd (%) | 66.19 | 63.35 | 58.45 | 75.33 |
| Coke deposition (g/g cat) | 1.03 | 0.30 | 0.58 | 0.68 |

[a] Reaction conditions: temperature, 260 °C; cold $H_2$ pressure, 1.0 MPa; 500 rpm; time: 3 h; 2.0 mL furfural + 2.0 mL acetic acid +0.3 g catalyst + 40.0 mL ethanol
[b] PtH, 5% Pt/HZSM-5; [c] PdH, 5% Pd/HZSM-5; [d] RuH, 5% Ru/HZSM-5; [e] PNH, 2% Pt 10% Ni/HZSM-5
AC, acetic acid conversion; FC, furfural conversion; Yd, total area percentage of desired products

Furthermore, furfural conversion increased to 73.56% when the bimetallic/HZSM-5 catalyst PNH was used. The cost of catalysts could be reduced in this way.

GC-MS results for the liquid products are displayed in Table 3. The products were composed of esters, furan derivatives, acetals, acids, and alcohols/ethers. Major compounds over different catalysts gave similar results. However, the distribution of products for PtH, PdH, RuH, and PNH was different. The relative content of 2-furaldehyde diethyl acetal over PdH and RuH was higher than that over PtH and PNH. 3-(2-furanyl)-2-propenal had a higher relative content over PtH and PNH, while 1,1-diethoxy ethane showed the opposite result. The highest relative content of 2-ethoxy methy furan was acquired over PdH, while its lowest value was obtained over PtH. 2-Furanmethanol, tetrahydro- was only detected with the catalysis of PdH. The highest relative content of 4-oxo-pentanoic acid ethyl ester and the lowest relative content of 2-furanmethanol was obtained over RuH. PNH had the lowest relative content of 4-oxo-pentanoic acid ethyl ester and the highest relative content of 2-furanmethanol and 2-methyl furan. In general, the relative content of furfural hydrogenation products and aldol condensation product (3-(2-furanyl)-2-propenal) was higher for PtH and PNH. The causes of the differences are discussed below. The Yd for different catalysts is shown in Table 2. The Yd for the employed catalysts followed the order: PNH > PtH > PdH > RuH. This was similar to furfural conversion, demonstrating the superior catalytic performance of PNH and PtH.

In the catalytic upgrading of bio-oil, coke deposition on catalysts presents a severe problem. As can be seen in Table 2, PtH showed the highest coke deposition, which was 1.03 g/g cat. Coke deposition for PdH and RuH was much lower, which was 0.30 g/g cat

and 0.58 g/g cat, respectively. The coke resistant ability of PtH improved significantly by adding Ni as a second metal. The coke deposition of PNH was 0.68 g/g cat.

**Table 3.** GC-MS Results of Liquid Products Using Different Catalysts [a, b]

| Compound Name | Relative Content (%) | | | |
|---|---|---|---|---|
| | PtH [c] | PdH [d] | RuH [e] | PNH [f] |
| *Acetals* | | | | |
| 1,1-diethoxy ethane | 3.82 | 6.63 | 9.03 | 1.60 |
| 5,5-diethoxy-2-pentanone | | 0.88 | 1.81 | |
| Acids | | | | |
| 2-naphthalenyloxy-acetic acid | | | | 1.91 |
| Alcohols/ethers | | | | |
| p-ethoxybenzyl alcohol | 0.97 | | 0.54 | |
| Ethyl ether | 0.84 | | 0.45 | |
| *Esters* | | | | |
| 4-oxo-pentanoic acid, ethyl ester | 14.11 | 7.98 | 15.88 | 6.07 |
| Ethyl acetate | 17.16 | 14.51 | 12.59 | 19.65 |
| Hexadecanoic acid, ethyl ester | | | | 1.15 |
| Furan derivatives | | | | |
| 2-ethoxy methyl furan | 15.53 | 27.84 | 21.56 | 23.66 |
| 2-furanmethanol | 12.44 | 8.14 | 4.90 | 14.15 |
| 3-(2-furanyl)-2-propenal | 10.96 | 2.44 | 2.47 | 7.81 |
| 2-furaldehyde diethyl acetal | 10.16 | 19.65 | 18.71 | 8.64 |
| 2-methyl furan, | 1.66 | 1.26 | 0.91 | 3.05 |
| 2-(2-furanylmethyl)-5-methyl furan | 1.21 | 0.66 | 0.61 | 1.87 |
| 2,2'-(1,2-ethenediyl)bis-, (E)-furan, | 1.22 | | | 2.71 |
| 2-furancarboxylic acid, ethyl ester | 1.14 | | 0.63 | 1.43 |
| 2-furanmethanol, tetrahydro- | | 2.17 | | |
| 2,2'-methylenebis furan | | 0.79 | 0.42 | |
| 5-methyl-2-furancarboxaldehyde | | 0.66 | 0.41 | |
| *Hydrocarbons* | | | | |
| Heptadecane | 0.76 | | | 1.59 |
| *Unidentified* | 8.03 | 6.40 | 9.09 | 4.70 |

[a] Reaction conditions: temperature, 260 °C; cold $H_2$ pressure, 1.0 MPa; 500 rpm; time, 3 h; 2.0 mL furfural + 2.0 mL acetic acid +0.3 g catalyst + 40.0 mL ethanol
[b] Ethanol and reactants were excluded; [c] PtH, 5% Pt/HZSM-5; [d] PdH, 5% Pd/HZSM-5; [e] RuH, 5% Ru/HZSM-5; [f] PNH, 2% Pt 10% Ni/HZSM-5

Upgrading reactions catalyzed by either metal sites or acid sites took place after furfural was absorbed on the catalysts. However, furfural and its reaction intermediates tend to polymerize and finally form coke, especially with the catalysis of acid catalysts (Zhang *et al*. 2010; Yemiş and Mazza 2011). Therefore, furfural conversion and coke deposition of the catalysts were correlated with the catalytic ability of the catalysts. Based on this assumption, the performance of different catalysts can be explained as follows: The higher furfural conversion and coke deposition of PtH might be attributed to the higher catalytic ability of PtH. For the bimetallic-acid catalyst PNH, more acid sites were covered as the total metal loading was increased to 12%. Additionally, Pt was more

dispersed in PNH, and Ni, as a second metal, also possessed hydrogenation activity, which enhanced the hydrogenation ability. Hence, higher catalytic activity and coke resistant ability could be expected for the bimetallic catalyst PNH.

## Reaction Pathways and Catalytic Mechanisms

Tang *et al.* proposed one-step hydrogenation esterification to convert aldehydes and acids to esters (Tang *et al.* 2008; Yu *et al.* 2011a, 2011b). However, the reactions of acetic acid with furfural or its intermediates were not evident in these experiments because there were no corresponding products detected. This may be due to the rapid esterification of acetic acid in supercritical ethanol, which prevented further reactions of acetic acid and furfural or its intermediates. Therefore, it is reasonable to analyze the reaction pathways of furfural and acetic acid separately.

Based on the GC-MS results, it could be concluded that 2-furanmethanol is an important intermediate product of furfural. Another experiment was conducted to explore the reaction pathways of 2-furanmethanol at 260 °C and 1.0 MPa cold $H_2$ pressure over PtH. The GC-MS result of this experiment is listed in the Appendix (Table S1). The reaction pathways for furfural are quite complicated. Based on the experimental results obtained in this work and in the literature (Itaya *et al.* 1998; Li *et al.* 2011b; Merlo *et al.* 2009; Zheng *et al.* 2006), a tentative reaction network of furfural and 2-furanmethanol is proposed in Fig. 3.

Furfural mainly underwent four reaction pathways: (1) through hydrogenation to 2-furanmethanol, (2) acetalization to form ethoxy(furan-2-yl)methanol, which could be further condensed to 2-furaldehyde diethyl acetal or dehydrogenated to 2-furancarboxylic acid ethyl ester, (3) reaction with acetaldehyde to produce 3-(2-furanyl)-2-propenal through aldol condensation, and (4) decarbonylation to form furan, which further went through ring opening, hydrogenation, and acetalization to form 1,1-diethoxy butane. The reaction pathways for 2-furanmethanol are summarized as follows: (1) through hydrogenation-ring opening, forming 4-oxopentanal, which further went through acetalization to produce 5,5-diethoxy-2-pentanone, (2) through hydration-ring opening forming 4-oxo-pentanoic acid which reacted with ethanol producing 4-oxo-pentanoic acid ethyl ester, (3) through etherification to form 2-ethoxy-methyl furan, (4) through hydrogenolysis producing 2-methyl furan, and (5) through isomerization forming 5-methyl-2(5H)-furanone, which could be further hydrogenated to dihydro-5-methyl-2(3H)-furanone. Etherification, hydration-ring opening, and hydrogenation-ring opening were predominant reaction pathways of 2-furanmethanol, while the others were minor reaction pathways.

Acetic acid mainly reacted with ethanol to form acetate ester through esterification. In addition to esterification and reactions with furfural and its intermediates, ethanol etherified to ethyl ether or dehydrogenated to acetaldehyde (de Lima *et al.* 2008), which further condensed to 1, 1-diethoxy ethane.

To investigate the catalytic mechanism, blank experiments without catalysts and over HZSM-5 were conducted with the same reaction conditions, and the GC-MS results are displayed in the Appendix (Table S2). Ethyl acetate, 1,1-diethoxy ethane, and 2-furanaldehyde diethyl acetal were identified as major products for these two cases. This demonstrated that esterification, acetalization, and ethanol dehydrogenation could occur without a catalyst. No product from furfural hydrogenation was detected except for a trace amount of 2-ethoxy-methyl furan. This demonstrated that 2-furanmethanol was

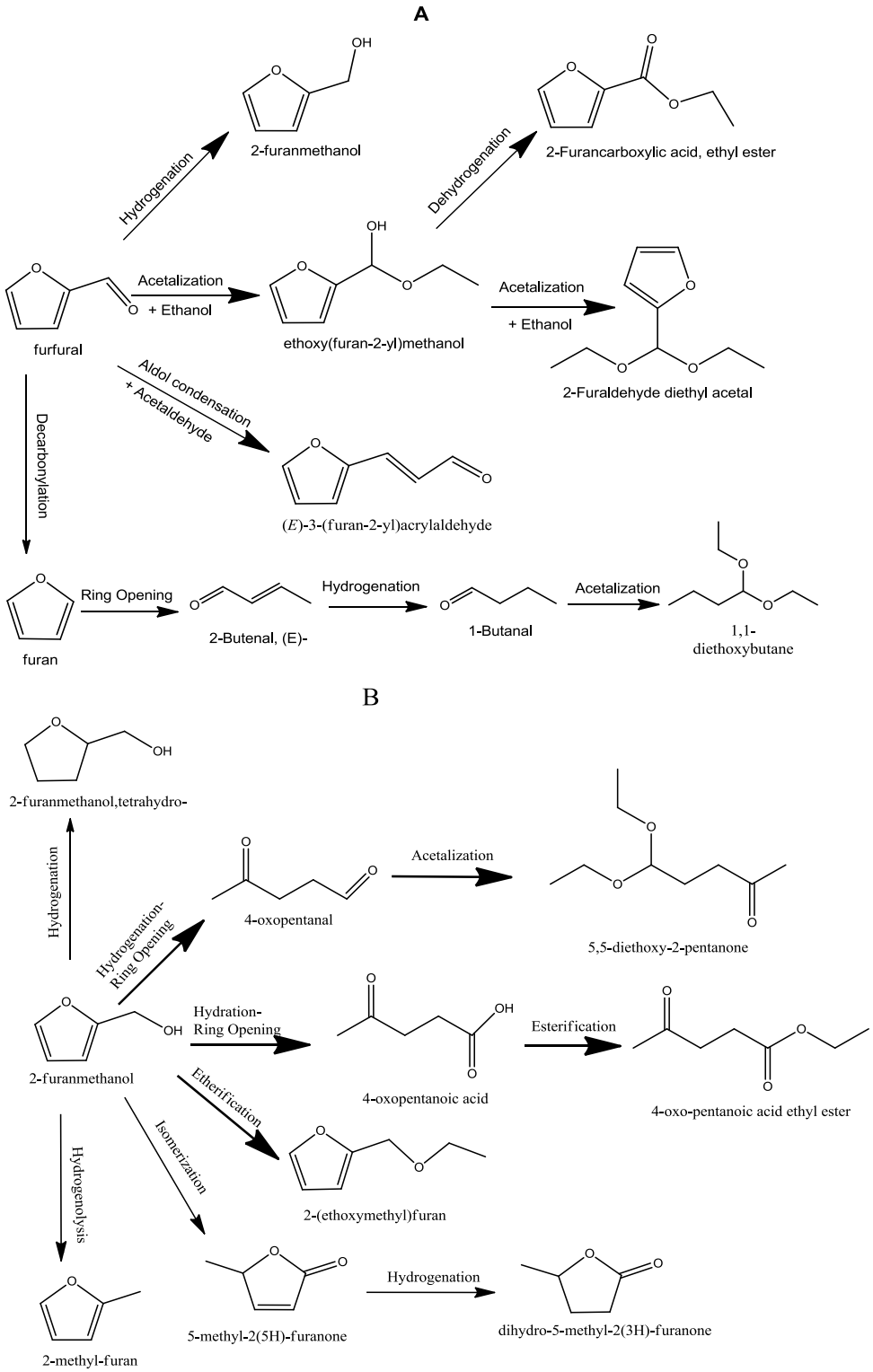


**Fig. 3.** Proposed reaction pathways of furfural and 2-furanmethanol. (A) Reaction pathways of furfural. (B) Reaction pathways of 2-furanmethanol

easily etherified even without a catalyst. The relative amount of ethyl ether was increased significantly over HZSM-5, indicating that HZSM-5 promoted the etherification of

ethanol. HZSM-5 might facilitate 2-furanmethanol hydration-ring opening, as 4-oxo-pentanoic acid ethyl ester was detected for the case over HZSM-5. For the cases over PtH, PdH, RuH, and PNH, the relative content of furfural hydrogenation products was much higher than the cases without catalysis or over HZSM-5. This demonstrated that impregnation with noble metal catalysts improved the furfural hydrogenation ability of catalysts. In addition, 3-(2-furanyl)-2-propenal was also observed over bifunctional catalysts, which indicated that these catalysts facilitated aldol condensation of furfural and acetaldehyde.

There were some differences in products distribution for these four bifunctional catalysts. The higher relative content of furfural hydrogenation products and 3-(2-furanyl)-2-propenal might be attributed to the higher catalytic ability of PtH and PNH. The detection of 2-furanmethanol, tetrahydro- over PdH might be due to the high C=C hydrogenation ability of Pd.

## Effects of Temperature and Cold $H_2$ Pressure

The effects of temperature and cold $H_2$ pressure were investigated in the range of 260 to 320 °C and 0.5 to 2.0 MPa. The default reaction conditions were set at 260 °C and 1.0 MPa. The effects of temperature on AC, FC, Yd, and coke deposition are presented in Fig. 4A. AC remained at 100% with increasing temperature. FC decreased slightly to 55.41% at 290 °C but increased significantly to 83.06% at 320 °C. Coke deposition presented the same tendency with temperature, reaching the minimum of 0.93 g/g cat at 290 °C and a maximum of 1.14 g/g cat at 320 °C. Yd declined to 48.55% at 290 °C and then rose to 57.06% at 320 °C. The GC-MS results of the liquid products under different reaction temperatures are listed in the Appendix (Table S3). The increase of relative content of 4-oxo- pentanoic acid ethyl ester in higher temperatures and the detection of 5,5-diethoxy-2-pentanone and 1,1-diethoxy- butane at 290 °C and 320 °C indicated that higher temperatures promoted the ring opening of furan. 1,1-diethoxy- butane and 2-butenal which might derive from furan, were detected at 320 °C, demonstrating that the decarbonylation of furfural occurred at 320 °C. The relative content of 1,1-diethoxy-ethane and ethyl ether, which were both derived from ethanol, increased significantly at higher reaction temperatures, demonstrating that higher reaction temperatures enhanced the self-reactions of ethanol. In conclusion, higher temperatures promoted furan ring opening and decarbonylation reactions and promoted self-reactions of ethanol. The slight decrease of FC at 290 °C might be attributed to the competitive adsorption of ethanol. In supercritical bio-oil upgrading, ethanol was mainly used as a reaction solvent and its excessive consumption was not expected. On the other hand, FC at lower reaction temperatures could be improved by catalyst amelioration. Thus, a lower reaction temperature was more suitable for this reaction system.

Figure 4B displays the effect of cold $H_2$ pressure on AC, FC, Yd, and coke deposition. Cold $H_2$ pressure had no effect on AC. FC increased from 35.26% to 62.94% as cold $H_2$ pressure increased from 0.5 MPa to 1.0 MPa, but then dropped to 37.28% at 2.0 MPa cold $H_2$ pressure. A similar tendency could be obtained for Yd and coke deposition. The influences of the initial $H_2$ pressure on products distribution (Table S3 in the Appendix) were complicated, and further research is still needed.

It can be concluded that AC was not influenced by reaction conditions, while FC varied significantly. From the results obtained, a lower reaction temperature and a moderate cold $H_2$ pressure are recommended.

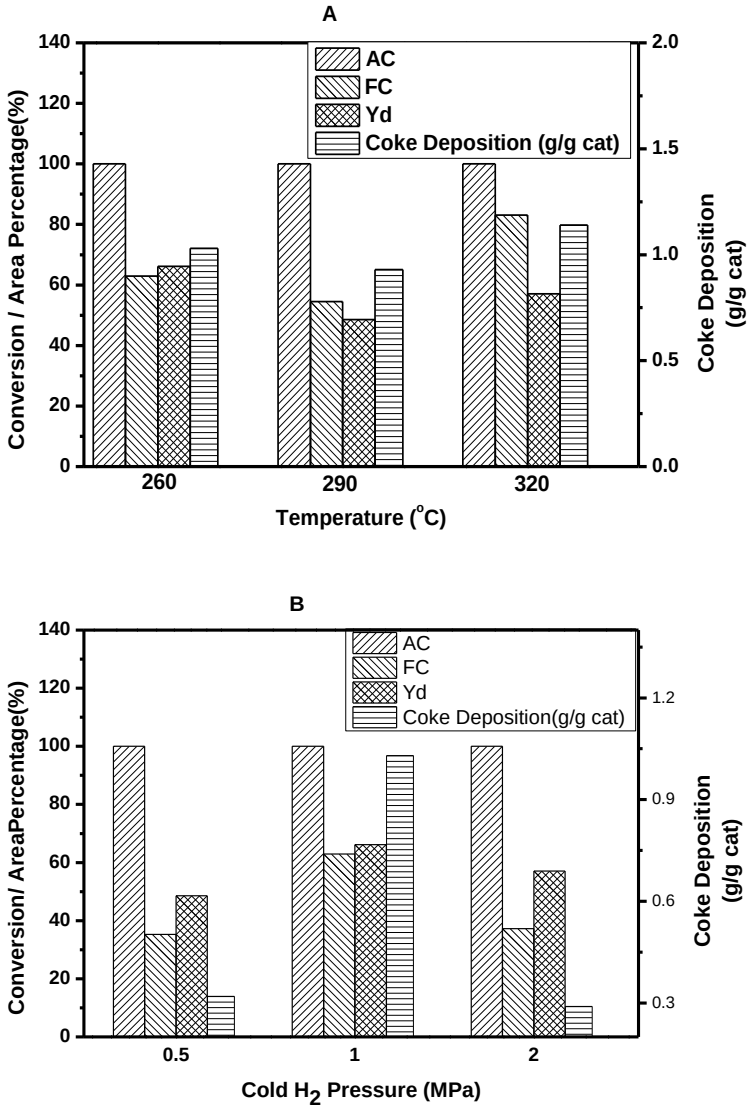


**Fig. 4.** Effects of temperature and cold $H_2$ pressure on AC, FC, Yd, and coke deposition. (A) Effects of temperature. (B) Effects of cold $H_2$ pressure. (Default reaction conditions: temperature, 260 °C; cold $H_2$ pressure, 1.0 MPa; 500 rpm; time: 3 h; 2.0 mL furfural + 2.0 mL acetic acid + 0.3 g catalyst + 40.0 mL ethanol)

## Effects of Other Typical Compounds in Bio-oil

Bio-oil is a complex mixture consisting of hundreds of organic compounds and water. The interactions of these compounds and their intermediates in bio-oil upgrading could not be neglected. Further work included adding 1 mL of water, acetone, and guaiacol to this reaction system separately to study the effects of water, ketones, and phenols on the upgrading process. The AC, FC, Yd, and coke deposition of upgrading reactions with different compounds are listed in Table 4.

AC remained 100%, while FC increased significantly to 79.29% with the addition of acetone. The increase of FC could be attributed to the aldol-crossed condensation of acetone and furfural, forming trans-furfurylideneacetone, as shown in Table S4 (see the Appendix). Yd and coke deposition increased as well with the addition of acetone. George Huber and others (Barrett *et al.* 2006; Huber *et al.* 2005) proposed a process in

which the aldol-crossed condensation of acetone and carbohydrate-derived aldehydes (mainly furfural or 5-hydroxymethylfurfural) was a key procedure to stretch the carbon chain to convert renewable biomass-derived carbohydrates into alkanes. In most studies (Di Cosimo *et al.* 1996; Xu *et al.* 2010; Zhang *et al.* 2003), solid base catalysts were used for aldol-crossed condensation. However, it also could be achieved using PtH in supercritical ethanol, as was verified in this study. In addition to aldol-crossed condensation, acetone also went through ketalization to 2,2-diethoxy propane, but to a much lower extent. The reaction of acetone with acetic acid could be neglected because there were no corresponding products detected. The relative content of 4-oxo-pentanoic acid ethyl ester, 3-(2-furanyl)-2-propenal, and 2-furaldehyde diethyl acetal decreased significantly, which indicated that aldol condensation of furfural and acetaldehyde, 2-furanmethanol hydration-ring opening and acetalization were inhibited after the addition of acetone.

With the addition of water, AC, FC, Yd, and coke deposition all decreased. AC and Yd decreased slightly to 90.6% and 58.75%, respectively, whereas FC and coke deposition decreased significantly to 26.78% and 0.24 g/g cat, respectively. In this reaction system, some reactions, such as esterification and acetalization, are equilibrium-driven reactions (Moens *et al.* 2009). The addition of water created an equilibrium limitation for these reactions and hence hindered the complete conversion of acetic acid and lowered furfural conversion. On the other hand, the competitive adsorption of water and furfural might be another reason for the drastic decrease of FC and coke deposition. After the addition of water, the relative content of 4-oxo-pentanoic acid ethyl ester increased to 25.27% (Table S4 in the Appendix), which demonstrated that hydration-ring opening became the most predominant reaction pathway for 2-furanmethanol. This might be due to an increase in the percentage of water in the reaction process.

Guaiacol had a negligible effect on AC, while FC and coke deposition decreased significantly to 36.84% and 0.30 g/g cat, respectively. Yd decreased slightly to 60.57%. Guaiacol was inactive under the circumstances, because no product of guaiacol was detected except a trace amount of 2-methyl phenol, as displayed in Table S4 (see the Appendix).

**Table 4.** Effects of Other Typical Compounds on AC, FC, Yd, and Coke Deposition [a]

| Compound Added | AC (%) | FC (%) | Yd (%) | Coke Deposition (g/g cat) |
|---|---|---|---|---|
| None | 100 | 62.94 | 66.19 | 1.03 |
| Acetone | 100 | 79.29 | 75.74 | 1.29 |
| Water | 90.6 | 26.78 | 58.75 | 0.24 |
| Guaiacol | 100 | 36.84 | 60.57 | 0.30 |

[a] Reaction conditions: temperature, 260 °C; cold $H_2$ pressure, 1.0 MPa, 500 rpm; time: 3 h; 2.0 mL furfural + 2.0 mL acetic acid + 1.0 mL other typical compounds + 0.3 g catalyst + 40.0 mL ethanol
AC, acetic acid conversion; FC, furfural conversion; Yd, total area percentage of desired products

From the results obtained in this section, it is reasonable to assume that the conversion of acids was mainly influenced by water content, and the conversion of aldehydes was sensitive to the composition of the bio-oil.

## CONCLUSIONS

1. The reaction of furfural and acetic acid was carried out in supercritical ethanol with metal–acid bifunctional catalysts. Acetic acids underwent esterification to form ethyl acetate.
2. The reaction pathway of furfural with 2-furanmethanol as an important intermediate product was also clarified. It was shown that it is possible to combine various reactions into one single process.
3. The effects of catalyst support and metal catalysts were discussed. It was concluded that esterification, acetalization, and ethanol dehydrogenation were mainly derived from thermal reactions. The formation of ethyl ether was facilitated by HZSM-5. Hydrogenation reactions and aldol condensation of furfural and acetaldehyde were promoted by metal catalysts (Pt, Pd, Ru, and Ni).
4. Pt-Ni/HZSM-5 had the best catalytic performance among the tested catalysts.
5. Higher temperatures promoted furan ring opening reactions and decarbonylation; the effect of the initial hydrogen pressure was complicated. Complete conversion of acetic acid was achieved, while the conversion of furfural was sensitive to reaction conditions and the presence of other model compounds.

## ACKNOWLEDGMENTS

This work was supported by the National Science and Technology Supporting Plan (Grant No. 2011BAD22B07) and the Major State Basic Research Development Program of China (2013CB228100).

## REFERENCES CITED

Ardiyanti, A. R., Gutierrez, A., Honkela, M. L., Krause, A., and Heeres, H. J. (2011). "Hydrotreatment of wood-based pyrolysis oil using zirconia-supported mono-and bimetallic (Pt, Pd, Rh) catalysts," *Applied Catalysis A: General* 407(1-2), 56-66.

Barrett, C. J., Chheda, J. N., Huber, G. W., and Dumesic, J. A., (2006). "Single-reactor process for sequential aldol-condensation and hydrogenation of biomass-derived compounds in water," *Applied Catalysis B: Environmental* 66(1-2), 111-118.

Czernik, S., and Bridgwater, A. V. (2004). "Overview of applications of biomass fast pyrolysis oil," *Energy & Fuels* 18(2), 590-598.

de Lima, S. M., da Cruz, I. O., Jacobs, G., Davis, B. H., Mattos, L. V., and Noronha, F. B. (2008). "Steam reforming, partial oxidation, and oxidative steam reforming of ethanol over Pt/$CeZrO_2$ catalyst," *Journal of Catalysis* 257(2), 356-368.

Di Cosimo, J. I., Diez, V. K., and Apesteguia, C. R. (1996). "Base catalysis for the synthesis of α,β-unsaturated ketones from the vapor-phase aldol condensation of acetone," *Applied Catalysis A: General* 137(1), 149-166.

Gayubo, A. G., Aguayo, A. T., Atutxa, A., Aguado, R., and Bilbao, J. (2004a). "Transformation of oxygenate components of biomass pyrolysis oil on a HZSM-5

zeolite I. Alcohols and phenols," *Industrial & Engineering Chemistry Research* 43(11), 2610-2618.

Gayubo, A. G., Aguayo, A. T., Atutxa, A., Aguado, R., Olazar, M., and Bilbao, J. (2004b). "Transformation of oxygenate components of biomass pyrolysis oil on a HZSM-5 zeolite. II. Aldehydes, ketones, and acids," *Industrial & Engineering Chemistry Research* 43(11), 2619-2626.

Huber, G. W., Chheda, J. N., Barrett, C. J., and Dumesic, J. A. (2005). "Production of liquid alkanes by aqueous-phase processing of biomass-derived carbohydrates," *Science* 308(5727), 1446-1450.

Itaya, H., Shiotani, A., and Toriyahara, Y. (1998). "Preparation of levulinic acid from furfuryl alcohol," *Japanese Patent*, 62252742.

Li, W., Pan, C., Sheng, L., Liu, Z., Chen, P., Lou, H., and Zheng, X. (2011a). "Upgrading of high-boiling fraction of bio-oil in supercritical methanol," *Bioresource Technology* 102(19), 9223-9228.

Li, W., Pan, C., Zhang, Q., Liu, Z., Peng, J., Chen, P., Lou, H., and Zheng, X. (2011b). "Upgrading of low-boiling fraction of bio-oil in supercritical methanol and reaction network," *Bioresource Technology* 102(7), 4884-4889.

Merlo, A. B., Vetere, V., Ruggera, J. F., and Casella, M. L. (2009). "Bimetallic PtSn catalyst for the selective hydrogenation of furfural to furfuryl alcohol in liquid-phase," *Catalysis Communications* 10(13), 1665-1669.

Moens, L., Black, S. K., Myers, M. D., and Czernik, S. (2009). "Study of the neutralization and stabilization of a mixed hardwood bio-oil. *Energy & Fuels* 23(5), 2695-2699.

Mortensen, P. M., Grunwaldt, J. D., Jensen, P. A., Knudsen, K. G., and Jensen, A. D. (2011). "A review of catalytic upgrading of bio-oil to engine fuels," *Applied Catalysis A: General* 407(1-2), 1-19.

Peng, J., Chen, P., Lou, H., and Zheng, X. (2008). "Upgrading of bio-oil over aluminum silicate in supercritical ethanol," *Energy & Fuels* 22(5), 3489-3492.

Peng, J., Chen, P., Lou, H., and Zheng, X. (2009). "Catalytic upgrading of bio-oil by HZSM-5 in sub- and super-critical ethanol," *Bioresource Technology* 100(3), 3415-3418.

Tang, Y., Yu, W., Mo, L., Lou, H., and Zheng, X. (2008). "One-step hydrogenation-esterification of aldehyde and acid to ester over bifunctional Pt catalysts: A model reaction as novel route for catalytic upgrading of fast pyrolysis bio-oil," *Energy & Fuels* 22(5), 3484-3488.

Tang, Z., Lu, Q., Zhang, Y., Zhu, X., and Guo, Q. (2009). "One step bio-oil upgrading through hydrotreatment, esterification, and cracking," *Industrial & Engineering Chemistry Research* 48(15), 6923-6929.

Wildschut, J., Mahfud, F. H., Venderbosch, R. H., and Heeres, H. J. (2009). "Hydrotreatment of fast pyrolysis oil using heterogeneous noble-metal catalysts," *Industrial & Engineering Chemistry Research* 48(23), 10324-10334.

Wildschut, J., Iqbal, M., Mahfud, F. H., Cabrera, I. M., Venderbosch, R. H., and Heeres, H. J. (2010). "Insights in the hydrotreatment of fast pyrolysis oil using a ruthenium on carbon catalyst," *Energy Environ. Sci.* 3, 962-970.

Xu, W., Liu, X., Ren, J., Zhang, P., Wang, Y., Guo, Y., Guo, Y., and Lu, G. (2010). "A novel mesoporous Pd cobalt aluminate bifunctional catalyst for aldol condensation and following hydrogenation," *Catalysis Communications* 11(8), 721-726.

Yemiş, O., and Mazza, G. (2011). "Acid-catalyzed conversion of xylose, xylan and straw into furfural by microwave-assisted reaction," *Bioresource Technology* 102(15), 7371-7378.

Yu, W., Tang, Y., Mo, L., Chen, P., Lou, H., and Zheng, X. (2011a). "Bifunctional Pd/Al-SBA-15 catalyzed one-step hydrogenation–esterification of furfural and acetic acid: A model reaction for catalytic upgrading of bio-oil," *Catalysis Communications* 13(1), 35-39.

Yu, W., Tang, Y., Mo, L., Chen, P., Lou, H., and Zheng, X. (2011b). "One-step hydrogenation–esterification of furfural and acetic acid over bifunctional Pd catalysts for bio-oil upgrading," *Bioresource Technology* 102(17), 8241-8246.

Zhang, Z., Dong, Y. W., and Wang, G. W. (2003). "Efficient and clean aldol condensation catalyzed by sodium carbonate in water," *Chemistry Letters* 32(10), 966-967.

Zhang Q., Chang J., Wang, T. J., and Ying, X. (2007). "Review of biomass pyrolysis oil properties and upgrading research," *Energy Conversion and Management* 48(1), 87-92.

Zhang, X. H., Wang, T. J., Ma, L. L., and Wu, C. Z. (2010). "Aqueous-phase catalytic process for production of pentane from furfural over nickel-based catalysts," *Fuel* 89(10), 2697-2702.

Zhang, J., Luo, Z., Dang, Q., Wang, J., and Chen, W. (2012). "Upgrading of bio-oil over bifunctional catalysts in supercritical monoalcohols," *Energy & Fuels* 26(5), 2990-2995.

Zheng, X., and Lou, H. (2009). "Recent advances in upgrading of bio-oils from pyrolysis of biomass," *Chinese Journal of Catalysis*, 30, 765-769.

Zheng, H. Y., Zhu, Y. L., Teng, B. T., Bai, Z. Q., Zhang, C. H., Xiang, H. W., and Li, Y. W. (2006). "Towards understanding the reaction pathway in vapour phase hydrogenation of furfural to 2-methylfuran," *Journal of Molecular Catalysis A: Chemical* 246(1-2), 18-23.

Article submitted: January 8, 2013; Peer review completed: April 2, 2013; Revised version received: May 26, 2013; Accepted: May 31, 2013; Published: June 4, 2013.

## APPENDIX

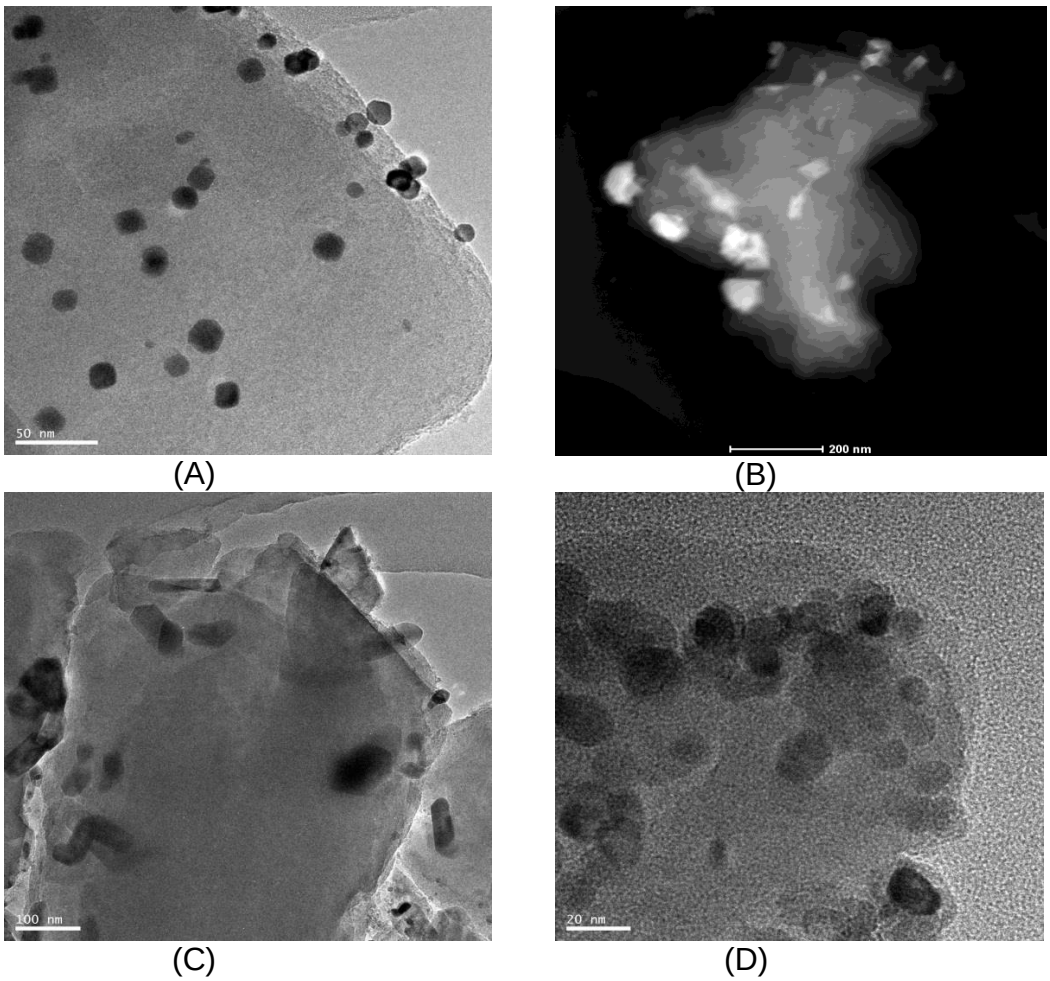


(A) (B)

(C) (D)

**Fig. S1.** STEM of the tested catalysts. (A) 5% Pt/HZSM-5; (B) 5% Pd/HZSM-5; (C) 5% Ru/HZSM-5; (D) 2% Pt-10% Ni/HZSM-5

**Table S1.** GC-MS Results of the Liquid Products of 2-furanmethanol in Supercritical Ethanol Using PtH [a]

| Compound Name | Relative Content (%) |
|---|---|
| 1,2-diethoxy ethane | 1.29 |
| 2-methyl furan | 1.21 |
| 1,1-diethoxy ethane | 4.57 |
| 3-furaldehyde | 0.70 |
| 2-ethoxy-methyl furan | 11.73 |
| 5-methyl-2(5H)-furanone | 1.01 |
| dihydro-5-methyl-2(3H)-furanone | 1.08 |
| 4-oxo-pentanoic acid ethyl ester | 64.73 |
| 2-furaldehyde diethyl acetal | 0.59 |
| 2,2'-methylenebis furan | 0.66 |
| 5,5-diethoxy-2-pentanone | 4.57 |
| 2-(2-furanylmethyl)-5-methyl-furan | 0.53 |
| Unidentified | 3.58 |

[a] Ethanol and 2-furanmethanol were excluded.
Reaction conditions: temperature: 260 °C; cold $H_2$ pressure, 1.0 MPa, 500 rpm; time: 3 h, 2.0 mL 2-furanmethanol + 0.3 g catalyst + 40.0 mL ethanol

**Table S2.** GC-MS Results of the Blank Experiments [a]

| Compound Name | Relative Content (%) | |
|---|---|---|
| | No Catalyst | HZSM-5 |
| Ethyl ether | | 24.05 |
| Ethyl acetate | 68.31 | 46.50 |
| 1,1-diethoxy-ethane | 13.91 | 10.63 |
| 2-ethoxy-methyl furan | 4.69 | 3.14 |
| ethoxy(furan-2-yl) methanol | 2.01 | 4.21 |
| 4-oxo-pentanoic acid ethyl ester | | 0.68 |
| 2-furaldehyde diethyl acetal | 11.19 | 10.79 |

[a] Ethanol and reactants were excluded.
Reaction conditions: temperature, 260 °C; cold $H_2$ pressure, 1.0 MPa, 500 rpm; time: 3 h, 2.0 mL furfural + 2.0 mL acetic acid + 0.3 g catalyst (or no catalyst) + 40.0 mL ethanol

**Table S3.** GC-MS Results of the Product in Different Reaction Conditions [a]

| Compound Name | Relative Content (%) | | | | |
|---|---|---|---|---|---|
| | Def [b] | 290 °C | 320 °C | 0.5 MPa | 2 MPa |
| *Acetals* | | | | | |
| 1,1-diethoxy ethane | 3.82 | 13.94 | 21.26 | 8.47 | 9.89 |
| 5,5-diethoxy-2-pentanone | | 4.96 | | | |
| 1,1-diethoxy butane | | | 4.36 | | |
| *Alcohols/ethers* | | | | | |
| Ethyl ether | 0.84 | 1.76 | 1.77 | 7.99 | 1.83 |
| p-ethoxybenzyl alcohol | 0.97 | | | | |
| Aldehydes | | | | | |
| 2-butenal, (E)- | | | 0.90 | | |
| *Esters* | | | | | |
| 4-oxo-pentanoic acid ethyl ester | 14.11 | 17.26 | 28.72 | 18.73 | 22.07 |
| Ethyl acetate | 17.16 | 9.01 | 10.03 | 15.58 | 10.05 |
| *Furan derivatives* | | | | | |
| 2-furancarboxylic acid, ethyl ester | 1.14 | | | | |
| 2-ethoxy-methyl furan | 15.53 | 18.43 | 7.15 | 15.18 | 13.97 |
| 2-furanmethanol | 12.44 | 1.28 | 0.31 | 2.43 | 2.75 |
| 3-(2-furanyl)-2-propenal | 10.96 | 1.89 | 1.53 | 1.44 | 2.14 |
| 2-furaldehyde diethyl acetal | 10.16 | 21.98 | 6.77 | 19.93 | 30.94 |
| 2-methyl furan, | 1.66 | 1.32 | 4.99 | 0.76 | 0.64 |
| 2-(2-furanylmethyl)-5-methyl furan | 1.21 | 0.67 | 2.23 | 0.52 | 0.45 |
| 2,2'-(1,2-ethenediyl)bis-, (E)-furan | 1.22 | | | | |
| 2,2'-methylenebis furan | | 0.57 | 1.62 | | 0.29 |
| 5-methyl-2-furancarboxaldehyde | | 0.31 | | 0.41 | 0.44 |
| Vinylfurans | | 0.31 | | 0.39 | 0.37 |
| 5-methyl-2(5H)-furanone | | | | | 0.72 |
| 2-ethyl furan | | | 0.65 | | |
| dihydro-5-methyl-2(3H)-furanone, | | | 1.36 | | |
| *Hydrocarbons* | | | | | |
| Heptadecane | 0.76 | | | | |
| Unidentified | 8.03 | 6.29 | 6.36 | 8.18 | 3.44 |

[a] Ethanol and reactants were excluded.
[b] Default reaction conditions: temperature: 260 °C; cold $H_2$ pressure, 1.0 MPa, 500 rpm; time: 3 h, 2.0 mL furfural + 2.0 mL acetic acid + 0.3 g catalyst (5% Pt/HZSM-5) + 40.0 mL ethanol

**Table S4.** GC-MS Results of the Liquid Products with the Addition of Other Typical Compounds in Bio-oil [a]

| Compound Name | Relative Content (%) | | | |
|---|---|---|---|---|
| | Def [b] | Ace [c] | Wat [d] | Gua [e] |
| *Acetals/ketals* | | | | |
| 1,1-diethoxy ethane | 3.82 | 3.35 | 7.9 | 7.84 |
| 2,2-diethoxy propane | | 0.66 | | |
| *Acids* | | | | |
| Ethyl hydrogen 4-oxoheptanedioate | | | 1.46 | |
| *Alcohols/ethers* | | | | |
| Ethyl ether | 0.84 | 0.8 | 2.06 | 2.16 |
| p-ethoxybenzyl alcohol | 0.97 | | | 0.48 |
| *Aldehydes* | | | | |
| 2,4-nonadienal, (E,E)- | | 2.62 | | |
| *Esters* | | | | |
| Ethyl acetate | 17.16 | 16.26 | 14.55 | 15.83 |
| 4-oxo-pentanoic acid ethyl ester | 14.11 | 5.15 | 25.27 | 15.60 |
| *Furan derivatives* | | | | |
| 2-furanmethanol | 12.44 | 8.65 | 6.10 | 4.15 |
| 2-ethoxy-methyl furan | 15.53 | 16.71 | 10.75 | 22.88 |
| 2-furancarboxylic acid, ethyl ester | 1.14 | 1.22 | | |
| 3-(2-furanyl)-2-propenal | 10.96 | 4.49 | 3.31 | 3.46 |
| 2-furaldehyde diethyl acetal | 10.16 | 5.65 | 17.74 | 15.79 |
| 2-methyl-furan | 1.66 | 1.28 | 0.85 | 0.66 |
| 2-(2-furanylmethyl)-5-methyl furan | 1.21 | 0.54 | 0.57 | |
| 5-methyl-2-furancarboxaldehyde | | | 0.58 | 0.32 |
| Furan, 2,2'-(1,2-ethenediyl)bis-, (E)- | 1.22 | | | |
| Vinylfurans | | | 0.36 | 0.45 |
| 2,2'-methylenebis furan | | | 0.29 | 0.53 |
| trans-furfurylideneacetone | | 25.93 | | |
| *Hydrocarbons* | | | | |
| Heptadecane | 0.76 | | | |
| *Phenols* | | | | |
| 1,3-naphthalenediol | | 1.35 | | |
| 2-methyl phenol, | | | | 1.04 |
| *Unidentified* | 8.03 | 5.34 | 8.20 | 8.22 |

[a] Ethanol and reactants were excluded.
[b] Def-default reaction conditions: temperature, 260 °C; cold $H_2$ pressure, 1.0 MPa, 500 rpm; time: 3 h, 2.0 mL furfural + 2.0 mL acetic acid + 0.3 g catalyst (5% Pt/HZSM-5) + 40.0 mL ethanol
[c] Another 1.0 mL acetone was added to the reaction mixture.
[fd] Another 1.0 mL water was added to the reaction mixture.
[e] Another 1.0 mL guaiacol was added to the reaction mixture.